RADIATIVE RECOMBINATION AND PHOTOIONIZATION CROSS SECTIONS FOR HEAVY ELEMENT IMPURITIES IN PLASMAS

M. B. Trzhaskovskaya
Department of Theoretical Physics
Petersburg Nuclear Physics Institute
Gatchina 188300, Russia

V. K. Nikulin
Division of Plasma Physics, Atomic Physics, and Astrophysics
A.F.Ioffe Physical-Technical Institute,
St.Petersburg 194021, Russia

R. E. H. Clark
Nuclear Data Section
International Atomic Energy Agency
Vienna A-1400, Austria

Research Co-ordination Meeting

on CRP

"Atomic data for heavy element impurities in fusion reactors"

IAEA, Vienna, Austria
26–28 September, 2007

1 INTRODUCTION

For the last two years, our goal was to produce a new unified database for the Radiative Recombination Cross Sections (RRCSs) and Photoionization Cross Sections (PCSs) as functions of the electron energy for a number of heavy element impurity ions occurring in plasmas. To date we calculated the subshell RRCSs and PCSs and total RRCSs for 31 ions of Fe, Ni, Cu, Mo, and W which are most important in fusion studies.

The ionic states of the heavy element impurities which are of the most importance in fusion study, are the following [4]:
(i) the fully stripped and H-like ions;
(ii) the most stable He-, Ne-, Ar-, and Kr-like ions with closed shells;
(iii) the Ni-like ion for molybdenum and tungsten as well as the Pd- and Er-like ions for tungsten.

As to point (iii), our calculations using the Dirac-Fock (DF) method, show the Ni-like ions with the standard configuration $3d^4_{3/2}3d^4_{5/2}4s^2$ as well as the Er-like ion W^{6+} with the standard configuration $4f^6_{5/2}4f^6_{7/2}6s^2$ to be metastable. The relevant ground states have closed the $3d$ shells, that is $[\mathrm{Ar}]\,3d^4_{3/2}3d^6_{5/2}$ and closed the $4f$ shell, that is $[\mathrm{Xe}]\,4f^6_{5/2}4f^8_{7/2}$. The total energy E_{total} calculated within the DF method for the Ni-like and Er-like ions as well as for the ions in the ground state are presented in Table 1 for the elements Kr, Mo, Xe, and W.

Table 1. Total energy of the Ni-like and Er-like ions as compared with electron configurations having closed shells

	$-E_{total}$, eV			
Ion	Closed shell	Ni-like	Er-like	Difference
Kr^{8+}	75396.0	75214.5		181.5
Mo^{14+}	108295.3	107859.6		435.7
Xe^{26+}	193702.8	192497.4		1205.4
W^{46+}	399294.0	396132.0		3162.0
W^{6+}	439443.0		439325.1	117.9

One can see that total energies for electron configurations with closed the $3d$ ($4f$) shells are considerably low than the relevant Ni-like and Er-like configurations. Because of that, we adopted 31 ions listed in Table 2.

Table 2. Recombining ion stages considered

	Ion charge				
Configuration	Fe	Ni	Cu	Mo	W
bare nucleus	26	28	29	42	74
H-like	25	27	28	41	73
He-like	24	26	27	40	72
Ne-like	16	18	19	32	64
Ar-like	8	10	11	24	56
$[\mathrm{Ar}]3d^4_{3/2}3d^6_{5/2}$				14	46
Kr-like				6	38
Pd-like					28
$[\mathrm{Xe}]4f^6_{5/2}4f^8_{7/2}$					6

The fully relativistic calculations were performed using the DF method where, as distinct from the Dirac-Slater (DS) method used in many previous papers, the exchange electron interaction was taken into account exactly, both for the bound electrons and between bound and free electrons. The calculations were carried out by the use of our computer code package RAINE [1, 2]. The numerical methods used in the codes, as well as the problem of the accuracy of calculations, were discussed at length in Refs. [1, 3]. It should be noted that PCS is calculated with a numerical precision of about 0.1%.

Subshell RRCSs and PCSs were computed for the ions in the ground and all excited electron states up to states with principal quantum number $n = 20$. Total RRCSs were calculated with regard to the contributions of all these states. The calculations were carried out for 41 values of the electron kinetic energy E_k from the range 4 eV$\leq E_k \leq$ 50 keV. Energy points are logarithmic over the range. Total RRCSs for the ions were published in tabular and graphical forms.

Subshell PCSs for ground and excited states with $n \leq 12$ and orbital quantum number $\ell \leq 6$ obtained in the calculations were fitted by a simple analytical expression with five fit parameters. The fit parameters for ~ 3300 electron states were also published.

Results obtained have been published in the following papers.

1. **M.B. Trzhaskovskaya, V.K. Nikulin, V.I. Nefedov and V.G. Yarzhemsky, Atomic Data and Nuclear Data Tables 92, 245–304, 2006.**
2. **M.B. Trzhaskovskaya, V.K. Nikulin, and R.E.H. Clark, "*Radiative recombination and photoionization cross sections for heavy element impurities in plasma: I. Tungsten ions. Theory*". PNPI Report, PNPI-2678, 36p. (2006).**
3. **M.B. Trzhaskovskaya, V.K. Nikulin, and R.E.H. Clark, "*Radiative recombination and photoionization cross sections for heavy element impurities in plasma: II. Tungsten ions. Tabulated results*". PNPI Report, PNPI-2679, 53p. (2006).**
4. **M.B. Trzhaskovskaya, V.K. Nikulin, and R.E.H. Clark, "*Radiative recombination and photoionization cross sections for heavy element impurities in plasmas: III. Ions of Iron, Nickel, and Copper. Tabulated results*". PNPI Report, PNPI-2699, 52 p. (2006).**
5. **M.B. Trzhaskovskaya, V.K. Nikulin, and R.E.H. Clark, "*Radiative recombination and photoionization cross sections for heavy element impurities in plasmas: IV. Molybdenum ions. Tabulated results*". PNPI Report, PNPI-2700, 28 p. (2006).**
6. **M.B. Trzhaskovskaya, V.K. Nikulin, and R.E.H. Clark, Atomic Data and Nuclear Data Tables, in press (2007).**
7. **M.B. Trzhaskovskaya and V.K. Nikulin, Phys. Rev. B 75, 177104 (2007).**

2 COMPARISON WITH RECENT DATABASES OF PCS AND RRCS

A number of the PCS and RRCS calculations are available, however, the majority of them are for the ground state of atoms and ions (see, for example, [5]-[11]).

More recent calculations underlying databases for PCSs and RRCSs for ground and excited states are listed in Table 3.

Table 3. Recent calculations of PCS and RRCS

Author	Method	Species	n_{max}	$n > n_{max}$	high-energy tail	L
S.N.Nahar and A.K.Pradhan, 2001-2006	Breit-Pauli; R-matrix; multiconf. expan.	$\gtrsim$50 ions	10	Kramers; hydro-gen	$E_0 = E_{th}$ largest, Kramers; fitting (2006) $\sigma_{ph} = \sigma^0_{ph}(E_0/E)^m$	dip
N.R.Badnell, 2006	multiconf. expan.; semi-rel. for $Z \geq$30	Z=1-30, 36,42,54 isoelect.seqs. up to Na-like	5	hydro-gen	$E_0 \approx 1.36Z^2$keV, $\sigma_{ph} \sim E^{-(3.5+\ell_i)}$	dip
M.F.Gu, 2003	DFS	$Z \leq 28$ isoelect.seqs. up to F-like	10	Kra-mers	$E_0 = 10E_{th}$ Extrapol.using Verner's fit param.	dip
D.A.Verner and G.J.Ferland, 1996	DFS (BT et al.) for grnd, semi-rel. (Clark et al.) for exct	Z = 1-30, H-, He-, Li-, Na-like ions	5	hydro-gen	grnd, $E_0 = 50$ keV exct, $E_0 = 10E_{th}$ Kramers at $10E_{th} \leq E \leq 100E_{th}$, $\sigma_{ph} \sim E^{-(3.5+\ell_i)}$ at $E \gtrsim 100E_{th}$	all L, grnd dip, exct
A.Ichihara and J.Eichler, 2000	rel.	Z=1-112 bare nucl.	3	–	$E_0 \gtrsim 1000$ keV	all L
M.Trzhaskovskaya, V.Nikulin, and R.E.H.Clark, 2006-2007	DF	Z=26-74 31 closed shell ions	20	–	$E_0 \approx 50$ keV	all L

Note. E_0 is the highest tabulated energy.
Abbreviations. "grnd" - ground state, "exct" - excited state, "hydrogen" - hydrogen-like approximation, "rel." - relativistic calculation.

Let us discuss the model used in our calculations as compared with the previous ones.

(i) In the majority of previous calculations, electron wave functions are computed using the Dirac-Fock-Slater (DFS) potential where the exchange between electrons is taken into account approximately [5]-[13] or even the Coulomb potential [12, 17]. However values of PCS (RRCS) obtained in the framework of the DFS method and the DF method where the exchange is taken properly into account, may significantly differ, especially for low-charged ions, to say nothing of calculations in the Coulomb potential. PCSs $\sigma^{(i)}_{ph}$ obtained within the DF method

(solid lines) and DFS method (dashed lines) for the $5d_{3/2}, 5f_{5/2}, 6s_{1/2}$, and $6p_{1/2}$ shells of the ion W^{5+} are shown in Fig. 1. These shells (along with appropriate fine-structure components) make a major contribution to the total RRCS for the corresponding recombining ion W^{6+}. As seen, there are significant differences between the two calculations.

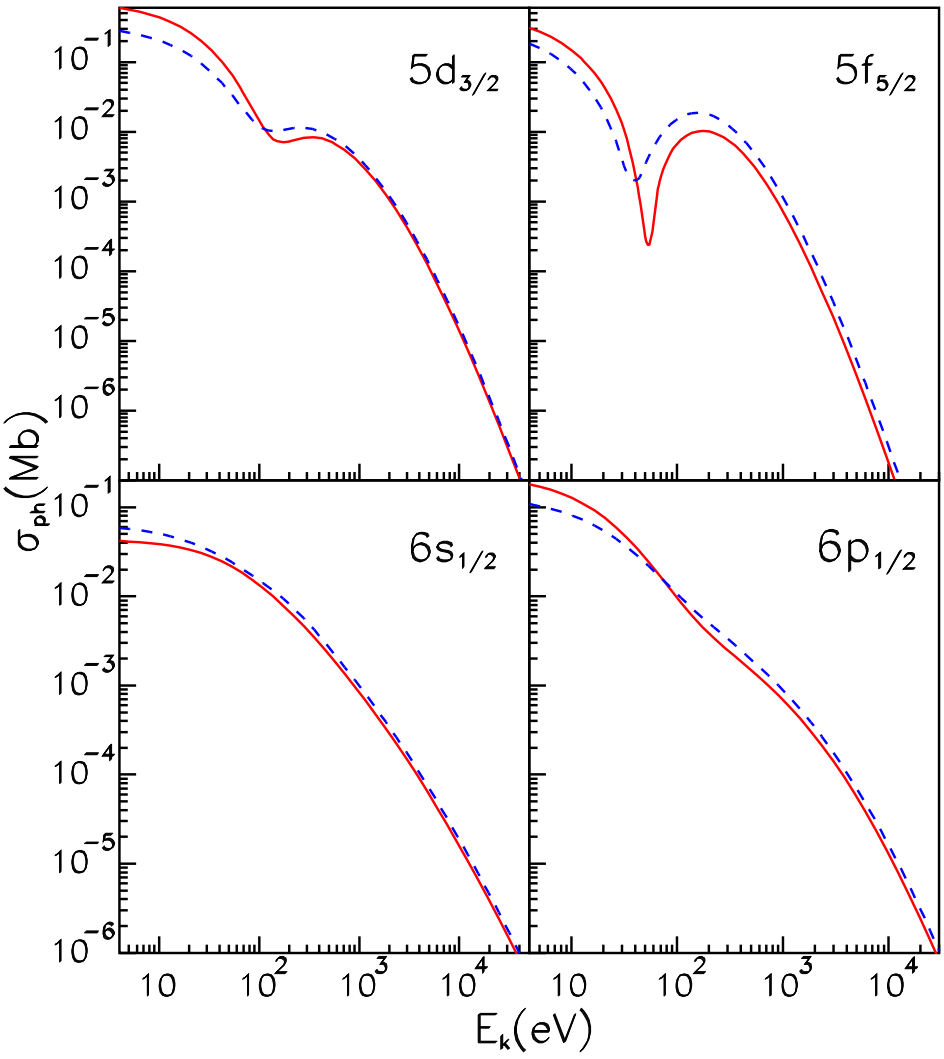

Figure 1: PCS $\sigma_{ph}^{(i)}$ (in Mb) versus the photoelectron energy E_k for various shells of the ion W^{5+}. Solid, DF calculation; dashed, DFS calculation.

Exact values of the difference

$$\Delta_{\rm mod} \;=\; \left[\frac{\sigma_{ph}({\rm DFS}) - \sigma_{ph}({\rm DF})}{\sigma_{ph}({\rm DF})}\right] \cdot 100\% \qquad (1)$$

are given in Table 4 for four energies in the range under consideration. As is seen, at the low photoelectron energy, the difference $\Delta_{\rm mod}$ is considerable. Even at the highest energy, 50.327 keV, the difference between the DFS and DF results are 17% for the $5d_{3/2}$ shell, 79% for $5f_{5/2}$, 18% for $6s_{1/2}$, and 28% for the $6p_{1/2}$ shell.

Table 4. Difference $\Delta_{\rm mod}$ (in %) in PCSs calculated by the use of the DFS and DF models for subshells of W^{5+}.

	Subshell			
E_k, eV	$5d_{3/2}$	$4f_{5/2}$	$6s_{1/2}$	$6p_{1/2}$
10.3	-53	-48	31	-36
109	-6	112	14	13
1153	13	61	19	28
50327	17	79	18	28

Due to these differences in the PCS and thus in RRCS values, the more accurate DF model should be preferred.

Note, that at the very low photoelectron energy, both the one-electron approximations may be not quite accurate due to possible influence of electron correlations. However the correlation effect is not expected to be substantial for photoionization of ions with the only electron above a closed core or for the He-like ions considered here. In Fig. 2, we compare our DF values of $\sigma_{ph}(E_k)$ with the relevant background nonresonant PSCs obtained by Nahar *et al.* [15, 16] using the Breit-Pauli R-matrix method where the electron correlations are taken into account. The comparison is given for available ions having a one electron above a closed core, namely for the Li-like ions. PCSs are presented for the $2s$ shell of the Ne^{7+} ion (Fig. 2(a)) and for the highly-charged Fe^{23+} ion (Fig.2(b)). As is clearly seen, our results are in good agreement with R-matrix calculations in the electron energy range under consideration. The average deviations of the DF values from PCSs obtained using the R-matrix method are 3.7% for Ne^{7+} and 1.6% for Fe^{23+}.

(ii) Another often-used approximation in the PCS calculations is the dipole one [14, 15, 16, 18] when only one term with L=1 is taken into account in Eq. (7) (see

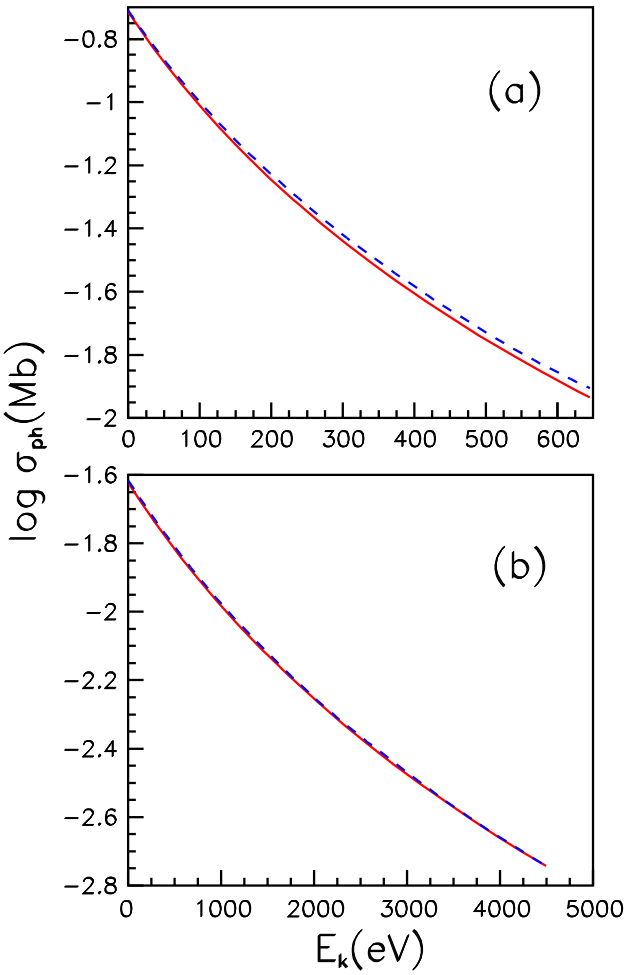

Figure 2: A comparison between $\sigma_{ph}(E_k)$ calculated within the DF method (solid) and the R-matrix method [15, 16] (dashed) for the $2s$ shell of the Li-like ions Ne^{7+} (a) and Fe^{23+} (b).

below). A comparison of RRCSs obtained in the dipole approximation $\sigma_{rr}(\mathrm{dip})$ and in the calculation involving all multipoles L of the radiation field $\sigma_{rr}(\mathrm{L})$, is given in Fig. 3 for bare nucleus in which case the difference Δ_{dip} between the two calculations is maximum.

A difference between the two calculations can be written as follows

$$\Delta_{\mathrm{dip}} = \frac{\sigma_{rr}(\mathrm{L}) - \sigma_{rr}(\mathrm{dip})}{\sigma_{rr}(\mathrm{L})} \cdot 100\%. \qquad (2)$$

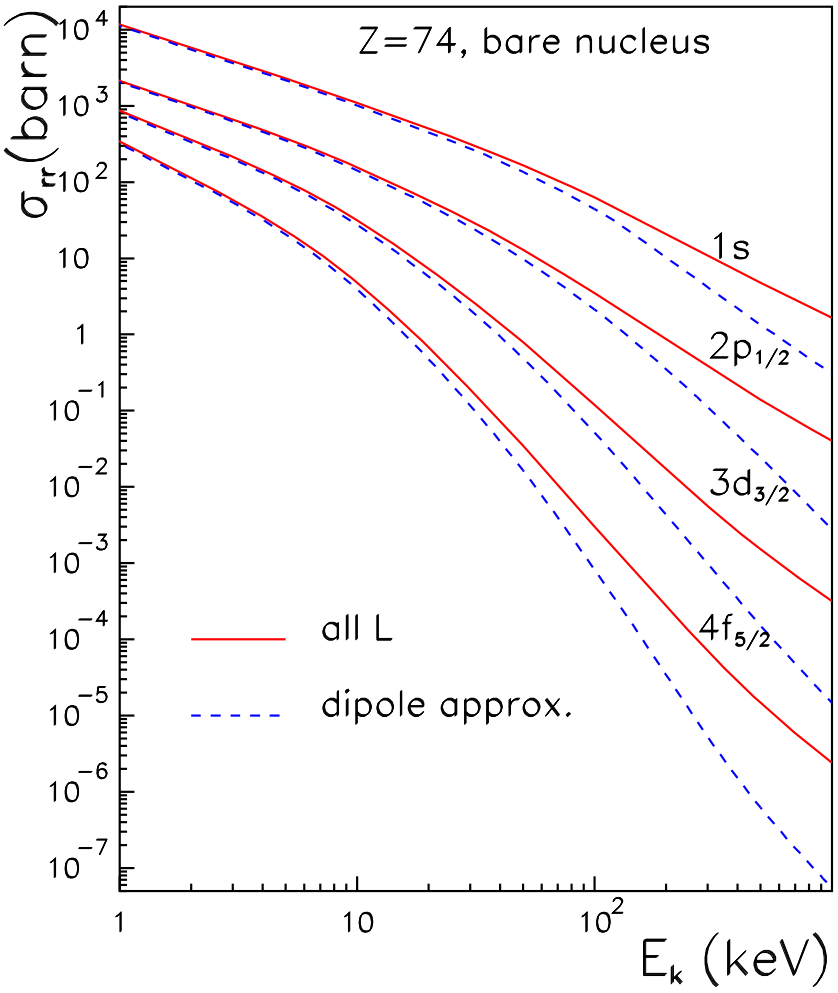

Figure 3: Subshell RRCSs (in barns) for the bare nucleus of W calculated taking into account all multipoles L (solid) and within the dipole approximation (dashed).

The difference $\Delta_{\rm dip}$ is given in Table 5 for several representative elements in the electron energy range 10 eV $\leq E_k \leq$ 1000 keV.

Table 5. Difference $\Delta_{\rm dip}$ (in %) between σ_{rr} calculated taking into account all multopoles $\sigma_{rr}(L)$ and in the dipole approximation $\sigma_{rr}(dip)$ (see Eq.(2)).

E_k,	$1s$ shell				$2p_{1/2}$ shell				$3d_{3/2}$ shell				$4f_{5/2}$ shell			
keV	Ne	Zn	Xe	W	Ne	Zn	Xe	W	Ne	Zn	Xe	W	Ne	Zn	Xe	W
0.01	0.1	0.8	2.3	3.6	0.1	0.7	1.9	2.6	0.1	0.7	2.0	2.9	0.1	0.7	2.0	3.1
1	0.4	1.2	3.2	5.4	0.7	1.4	3.1	4.7	1.1	3.8	3.5	5.5	1.7	2.4	4.0	6.1
10	3.2	4.0	5.8	7.9	5.6	6.4	7.7	8.9	10	10	12	13	15	15	16	18
50	15	15	17	18	24	24	25	24	38	38	38	38	51	52	52	52
100	27	27	28	29	40	40	40	39	58	58	57	57	75	73	73	73
500	75	74	74	72	84	84	84	82	89	89	90	90	93	94	95	95
1000	83	83	82	82	92	93	93	93	93	94	95	95	98	97	97	98

As is shown, the dipole approximation differ from the exact calculations by $\sim 10\%$ for E_k=10 keV, $\sim 50\%$ for E_k=50 keV which is the highest energy under consideration in our work, and $\gtrsim 90\%$ for E_k=1000 keV which is close to the highest energy considered in paper [18]. Because of this, PCSs and RRCSs at high electron energies obtained within the dipole approximation are inaccurate.

(iii) Because the proper PCS calculation at high energy is a challenging task, the authors extrapolate PCSs obtained at lower energies [15] or add asymptotic values [12, 18] using the well-known expression derived in the nonrelativistic dipole approximation which is written as

$$\sigma_{ph}^{(i)} \sim k^{-(3.5+\ell_i)}, \tag{3}$$

where k is the photon energy and ℓ_i is the orbital momentum of the $i-th$ shell.

However, Eq.(3) breaks down for the asymptotic behavior of the relativistic PCS with regard to all multipoles L. Badnell [18] presents PCSs calculated in the dipole approximation for the $3s$ shell of the Mg^+ ion (Fig. 3 from [18]) multiplied by $k^{3.5}$. He writes that the product $\sigma_{ph}^{(3s)} \times k^{3.5}$ reaches an asymptotic value in the energy range $\lesssim$30 keV while the same product involving the DFS results [10, 11] presented by Verner grows with energy rapidly and has no asymptote in the range.

We present in Fig. 4 $\sigma_{ph} \times k^{3.5}$ by Badnell (taken from the paper) together with our calculations performed within the DFS and DF methods.

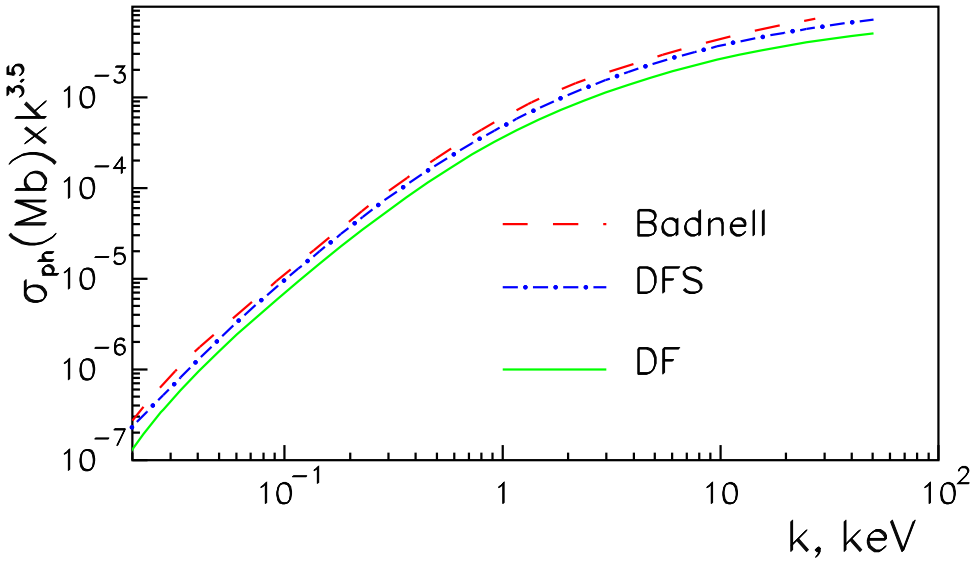

Figure 4: PCS multiplied by $k^{3.5}$ for the $3s$ shell of Mg^+. Solid, DF calculation; dashed, calculation by Badnell [18]; dot-dashed, our DFS calculation.

As is seen, all curvers are of a similar nature but the absolute values of $\sigma_{ph} \times k^{3.5}$ are somewhat different. It means that the comparison by Badnell is not true because the results by Verner are based on our DFS calculations. Besides, at first glance, all curves approach to asymptotic values, which they are not as is evident from Fig. 5.

In Fig. 5(a), the product $\sigma_{ph}^{(3s)} \times k^{3.5}$ is shown for the same case, $\sigma_{ph}^{(3s)}$ being calculated exactly (solid curve) and within the dipole approximation (dashed curve). As is seen, the solid curve has no asymptote at all in the energy range $k \leq$1000 keV. The dashed curve runs into an approximate asymptote. However the asymptote has little in common with real values of the product considered (compare solid and dashed curves).

In Fig. 5(b), the product involving the another power of the photon energy $\sigma_{ph}^{(3s)} \times k^{2.2}$ is shown. The value 2.2 was obtained by us using a fitting of the $\sigma_{ph}^{(3s)}$ values at lower energy. It holds for the s shells with various n of different elements and different ions. In this case, the solid curve associated with relativistic calculations with regard to all multipoles, reaches a good asymptote, even if at rather high energy $k \approx$ 300-400 keV. It should be noted that in the ultrarelativistic limit m =1 [20]. In Fig. 5(c), the exact PCS (solid) and PCS obtained in the dipole approximation (dashed) are displyed for the same case.

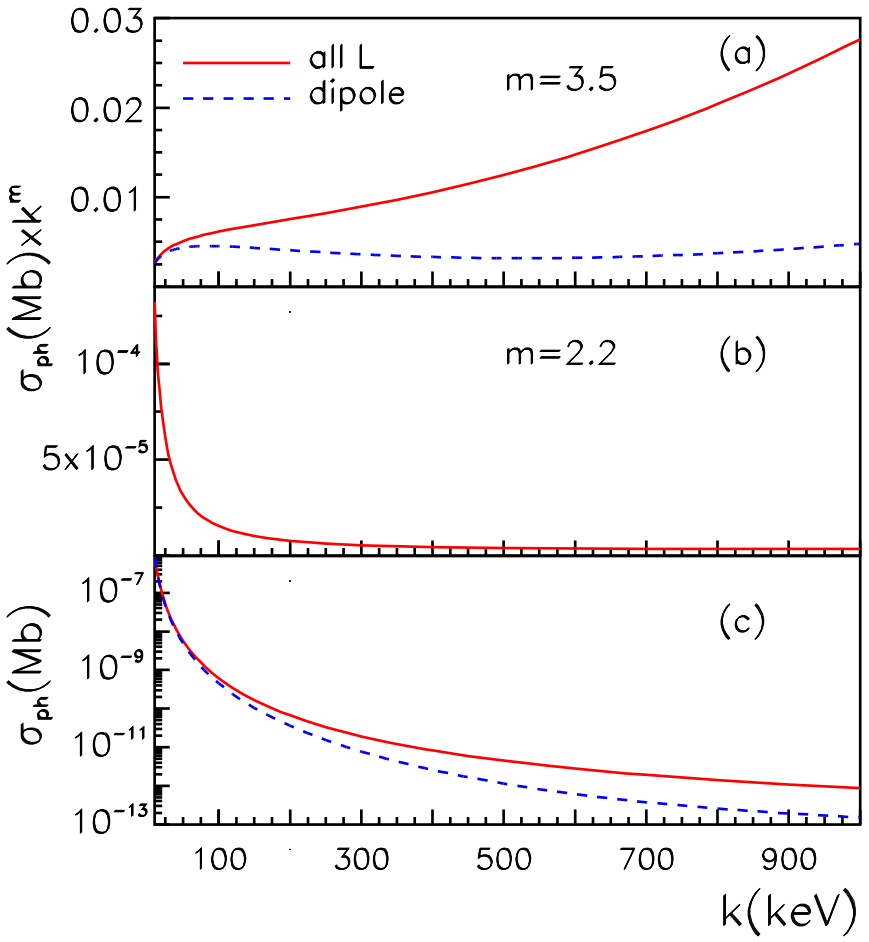

Figure 5: PCS multiplied by k^m where $m = 3.5$ (a) and $m = 2.2$ (b) and PCS (c) for the $3s$ shell of Mg^+. Solid, DF calculation having regard to all multipoles L; dashed, the DF dipole approximation.

(iv) To find the total RRCS, the direct calculations are usually carried out for excited states with n_{max} ≤10 only. However, for fusion plasmas with electron density in the range of $10^{14}/\mathrm{cm}^3$, an upper limit to the principal quantum number is $n \approx 20$. Because of this, excited states with higher than n_{max} are taken into account by the use of the H-like approximation [12] or with the Kramers formula [13, 14, 16]. We present in Fig. 6 the difference Δ_{add} between additional sums $\sum_{n=11}^{20} \sigma_{rr}$ where RRCS is calculated within the DF method $\sigma_{rr}(\mathrm{DF})$ and with the Kramers formula $\sigma_{rr}(\mathrm{Kram})$. The difference can be written as

$$\Delta_{\mathrm{add}} = \frac{\sum_{n=11}^{20} \sigma_{rr}(\mathrm{DF}) - \sum_{\mathrm{n=11}}^{20} \sigma_{\mathrm{rr}}(\mathrm{Kram})}{\sum_{n=11}^{20} \sigma_{rr}(\mathrm{DF})} \cdot 100\% \qquad (4)$$

Fig. 6 demonstrates that Δ_{add} reaches $\sim 100\%$ for the low-charged ion W^{6+}.

To be more precise, σ_{rr}(Kram) is by several orders less than σ_{rr}(DF) in this case. The difference decreases with increasing the ion charge. For the H-like ion of W (W^{73+}), maximum $\Delta_{\rm add}$ is equal 20%. Having regard to the contribution of the additional sum to the total RRCS ($\sim 10-15\%$), one can conclude that an approximate consideration of terms with high n using the Kramers formula may give rise the error in values of the total RRCS of the same order.

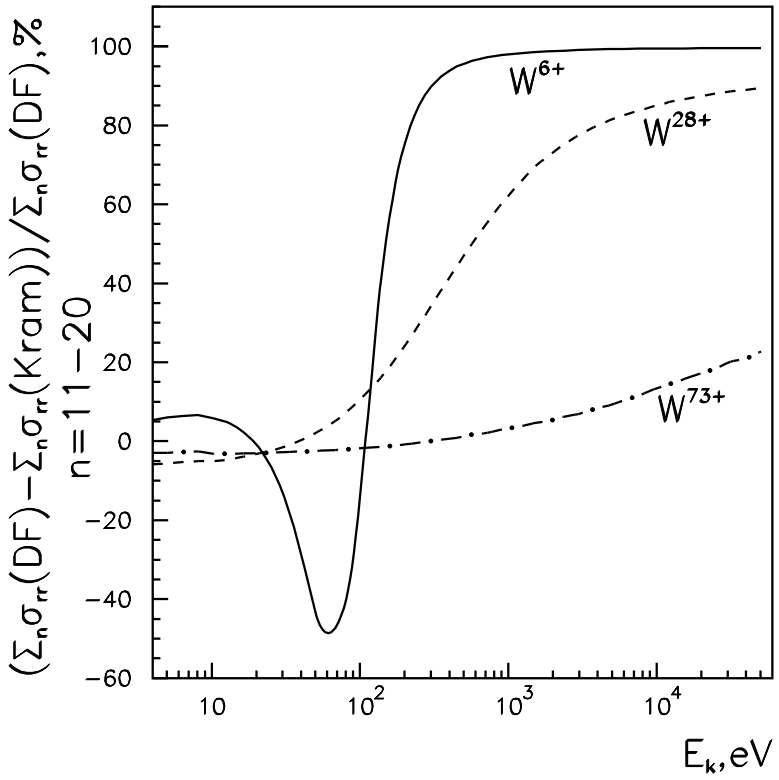

Figure 6: Difference $\Delta_{\rm add}$ (in %) between sums $\sum_{n=11}^{20}\sigma_{rr}$ calculated within the DF method and with the Kramers formula for ions of W.

(v) Finally, there exists the another effect which may also give rise an error in a partial RRCS at a high energy. All authors listed in Table 3 with the exception of Ichihara and Eichler used the transfer coefficient between PCS and RRCS in the form

$$\sigma_{rr}^{(i)} \;=\; \frac{k^2 q_v}{2E_k}\,\sigma_{ph}^{(i)}\;, \tag{5}$$

where q_v is the number of vacancies in the i-th subshell prior to recombination. Relativistic units ($\hbar = m_0 = c = 1$) are used. However the exact relativistic expression for the transfer coefficient is the following [17]

$$\sigma_{rr}^{(i)} \;=\; \frac{k^2 q_v}{2E_k + E_k^2}\,\sigma_{ph}^{(i)}\,. \tag{6}$$

It is clearly seen that adoption of the approximate Eq. (5) instead Eq. (6) leads to considerable errors at high energy – 4.7% at $E_k = 50$ keV, 8.9% at $E_k = 100$ keV, and 49.5% at $E_k = 1000$ keV.

Taking into consideration points (i)-(v), we believe that our calculations of partial and total RRCS and PCS are accurate within the one-electron model and offer certain advantages over other approaches.

3 METHOD OF CALCULATION

The basic formulas for the PCS calculations are the following.

The subshell PCS in the i-th subshell can be written in the form

$$\begin{aligned}\sigma_{ph}^{(i)} \;&=\; \frac{4\pi^2\alpha}{k(2j_i+1)}\sum_L\sum_\kappa\Big[(2L+1)Q_{LL}^2(\kappa) + LQ_{L+1L}^2(\kappa) \\ &+\; (L+1)Q_{L-1L}^2(\kappa) - 2\sqrt{L(L+1)}\,Q_{L-1L}(\kappa)Q_{L+1L}(\kappa)\Big]\;.\end{aligned} \tag{7}$$

Here L is the multipolarity of the radiation field, $\kappa = (\ell - j)(2j+1)$ is the relativistic quantum number, j is the total angular momentum of the electron, and α is the fine structure constant. The reduced matrix element $Q_{\Lambda L}(\kappa)$ is determined by the expression

$$\begin{aligned}Q_{\Lambda L}(\kappa) \;&=\; \big([\bar{\ell}][\ell_i]/[\Lambda]\big)^{1/2}\,C^{\Lambda 0}_{\bar{\ell}0\ell_i 0}\,\mathcal{A}\begin{pmatrix}\bar{\ell} & 1/2 & j\\ \ell_i & 1/2 & j_i\\ \Lambda & 1 & L\end{pmatrix}R_{1\Lambda} \\ &+\; \big([\ell][\bar{\ell}_i]/[\Lambda]\big)^{1/2}\,C^{\Lambda 0}_{\ell 0\bar{\ell}_i 0}\,\mathcal{A}\begin{pmatrix}\ell & 1/2 & j\\ \bar{\ell}_i & 1/2 & j_i\\ \Lambda & 1 & L\end{pmatrix}R_{2\Lambda}\;,\end{aligned} \tag{8}$$

where $\bar{\ell} = 2j - \ell$, $C^{\Lambda 0}_{\ell_1 0 \ell_2 0}$ is the Clebsch–Gordan coefficient, $\mathcal{A}\begin{pmatrix} \ell_1 & 1/2 & j_1 \\ \ell_2 & 1/2 & j_2 \\ \Lambda & 1 & L \end{pmatrix}$ is the recoupling coefficient for the four angular momenta, $[a]$ denotes the expression $(2a+1)$, $R_{1\Lambda}$ and $R_{2\Lambda}$ are the radial integrals in the form

$$\begin{aligned} R_{1\Lambda} &= \int_0^\infty G_i(r)F(r)j_\Lambda(kr)dr \ , \\ R_{2\Lambda} &= \int_0^\infty G(r)F_i(r)j_\Lambda(kr)dr \ . \end{aligned} \tag{9}$$

In Eq. (9), $j_\Lambda(kr)$ is the spherical Bessel function of the Λ-th order, $G(r)$ and $F(r)$ are the large and small components of the Dirac electron wave function multiplied by r. In Eqs. (7)-(9), the subscript i is related to the bound electron while designations with no subscript are related to the continuum spectrum electron. Electron wave functions are calculated in the framework of the DF method, that is, the bound and continuum wave functions represent the solutions of the DF equations with exact consideration of the exchange interaction [1, 19]. Both bound and continuum wave functions are calculated in the self-consistent field of the corresponding ions with $N+1$ and N electrons, respectively.

The subshell $\sigma^{(i)}_{rr}$ is determined by the use of Eq. (5) or Eq. (6). Summing subshell RRCSs $\sigma^{(n\kappa)}_{rr} \equiv \sigma^{(i)}_{rr}$ over all bound unfilled states, one arrives at the total RRCS which can be written as

$$\sigma^{tot}_{rr} = \sum_{n=n_{\min}}^{\infty} \sum_{\kappa=\mp 1,\mp 2,\ldots,-n} \sigma^{(n\kappa)}_{rr} \ , \tag{10}$$

where $n_{\min}$ combined with the appropriate value of κ refers to the ground state of the recombined ion.

The terms of the sum over κ in Eq. (10) decrease rather rapidly as κ increases. The higher the energy E_k, the more rapidly it decreases. Contributions of the terms corresponding to various orbital quantum numbers ℓ with respect to the total RRCS are plotted in Fig. 7 for three ions and four values of $E_k = 4$, 109, 1153, and 9646 eV, that is, we present the magnitude Δ_ℓ which can be written as

$$\Delta_\ell = \left[\sigma^{(\ell)}_{rr}/\sigma^{tot}_{rr}\right] \cdot 100\% \, , \tag{11}$$

where

$$\sigma^{(\ell)}_{rr} = \sum_{n=n_{min}}^{20} (\sigma^{(n\,\kappa=\ell)}_{rr} + \sigma^{(n\,\kappa=-\ell-1)}_{rr}). \tag{12}$$

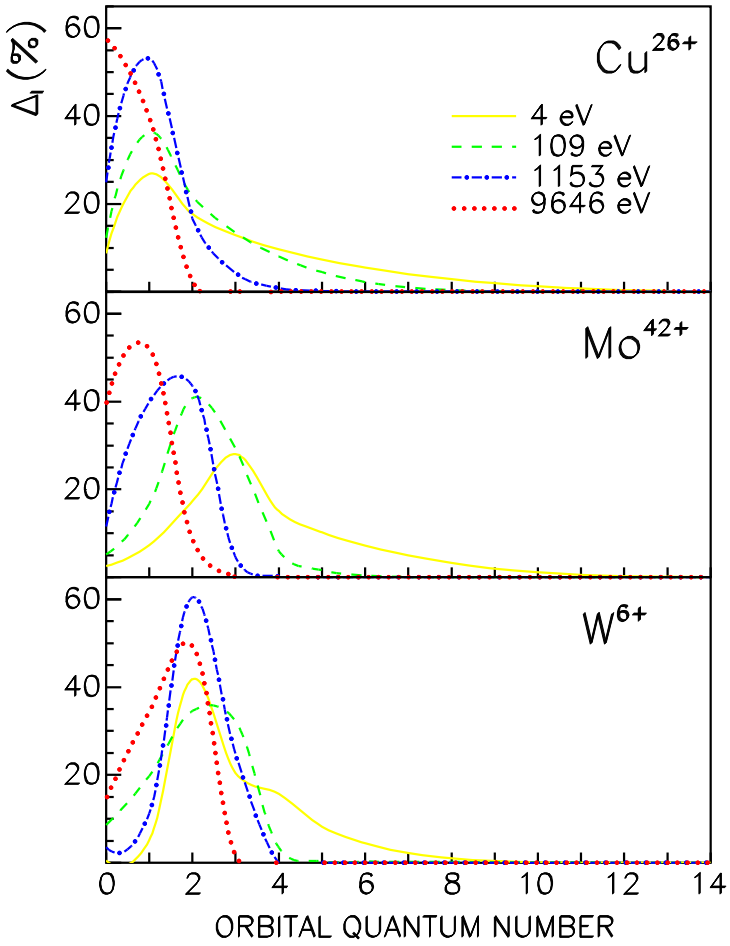

Figure 7: Contribution Δ_ℓ (in %) of terms $\sigma_{rr}^{(\ell)}$ to the total RRCS (Eqs. (11),(12)) for four values of the electron kinetic energy E_k.

As is evident, in all cases $\sigma_{rr}^{(\ell)}$ with large value of $\ell \gtrsim 8$ do not contribute significantly to σ_{rr}^{tot}. With regard to the rapid convergence of the sum over κ and a finite number of terms, we made allowance only for those values of κ which make a contribution to σ_{rr}^{tot} larger than 0.01%. Notice that fit parameters for subshell PCSs are given for shells with $\ell \leq 6$.

A different situation exists in summation of the infinite series over n in Eq. (10). Relative contributions of the states with various n to the total RRCS

$$\Delta_n \;=\; \left[\sigma_{rr}^{(n)}/\sigma_{rr}^{tot}\right]\cdot 100\%, \tag{13}$$

where

$$\sigma_{rr}^{(n)} \;=\; \sum_{\kappa=\mp 1,\mp 2\ldots -n} \sigma_{rr}^{(n\kappa)} \tag{14}$$

are given in Fig. 8 for the Ne-like ions Cu^{19+}, Mo^{32+}, and W^{64+} and for the same

four energies E_k. We see that Δ_n decreases rapidly at $n \lesssim 8$ but there is no rapid convergence at higher n. Although the contributions Δ_n for the largest value $n = 20$ do not exceed several percent, the tails of all curves in Fig. 8 decrease very slow – the lower E_k, the slower the decrease. So in the general case, the remainder of the infinite series in Eq. (10) should be taken into consideration.

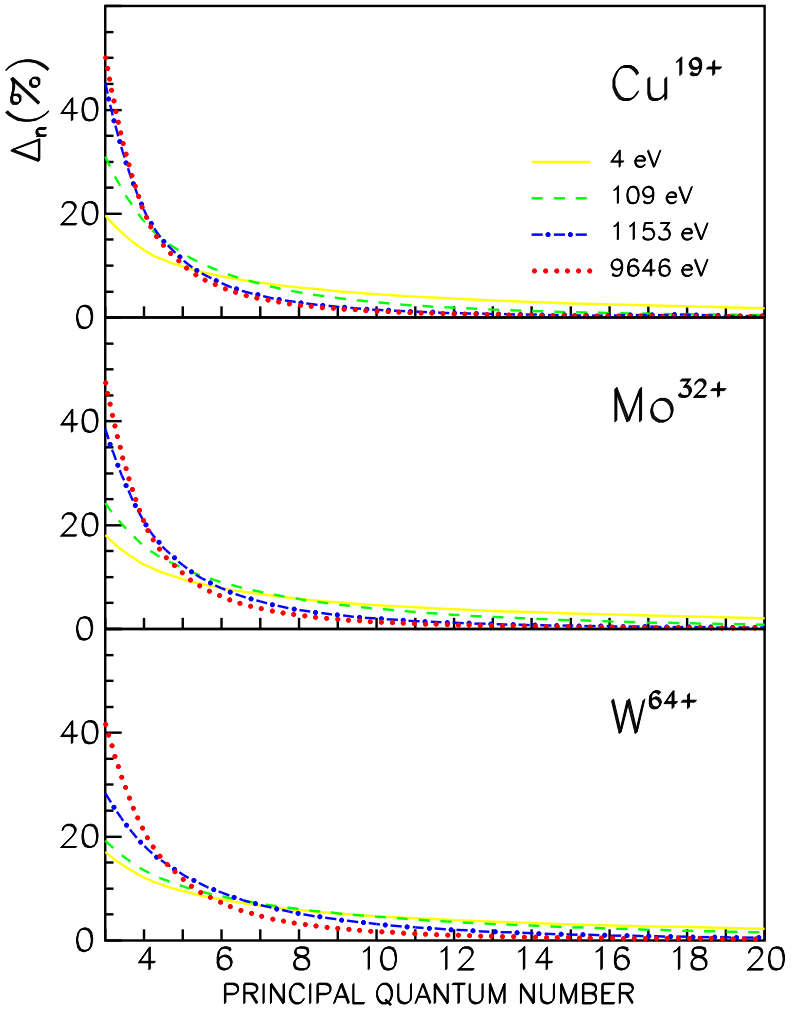

Figure 8: Convergence of the infinite series over n (Eq. (10)) in the form of contributions Δ_n (in %) of terms $\sigma_{rr}^{(n)}$ to the total RRCS (Eqs. (13),(14)) for four values of the electron kinetic energy E_k.

In a real plasma, however, there is a cutoff of bound levels from density effects, above which recombination is not meaningful. For fusion plasmas with electron density in the range of $10^{14}/\text{cm}^3$, the upper limit on the quantum number n is ≈ 20. Therefore the correction associated with the remainder of the infinite series in Eq. (10) is not required in fusion plasmas.

The electron energy dependence of the total RRCS is plotted in Figs. 9 -11 for recombining ions under consideration. One can see that the energy dependence $\sigma_{rr}^{tot}(E_k)$ exhibits minimum and maximum for the lowest-charged ions Mo^{6+} and W^{6+} because of a behavior of RRCSs for the lowest shells making a major contribution into σ_{rr}^{tot} (see Fig. 1). For higher-charged ions, the E_k-dependence presents smooth monotone curves.

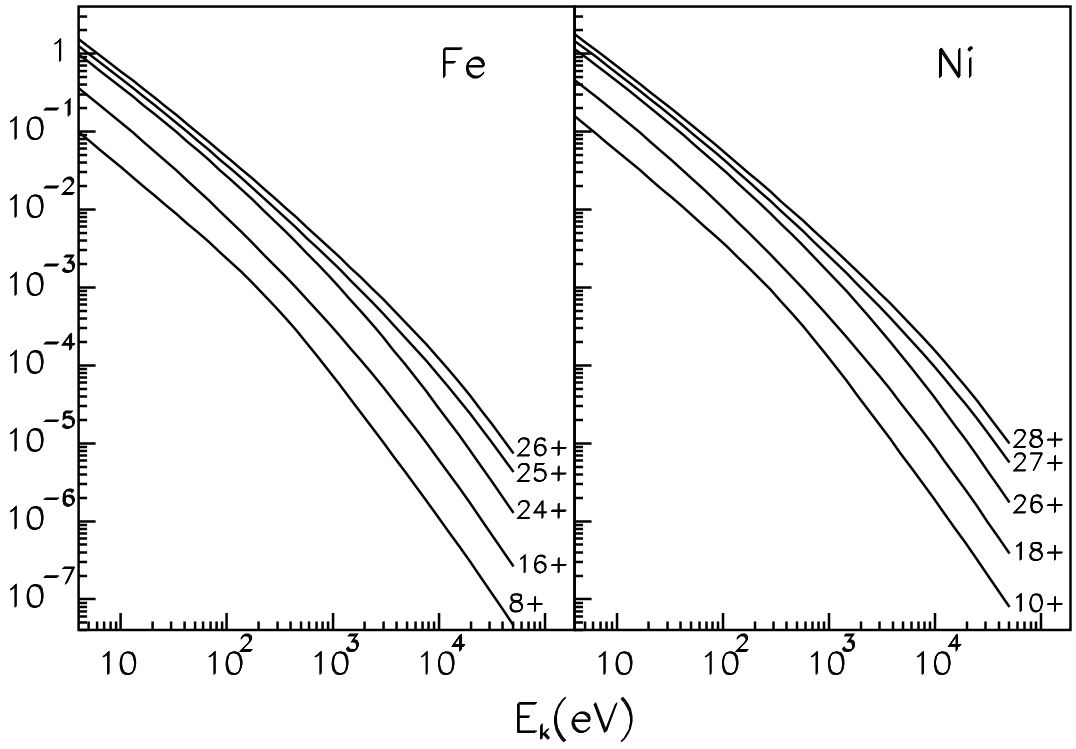

Figure 9: Total RRCS in Mb for ions of Fe and Ni versus E_k.

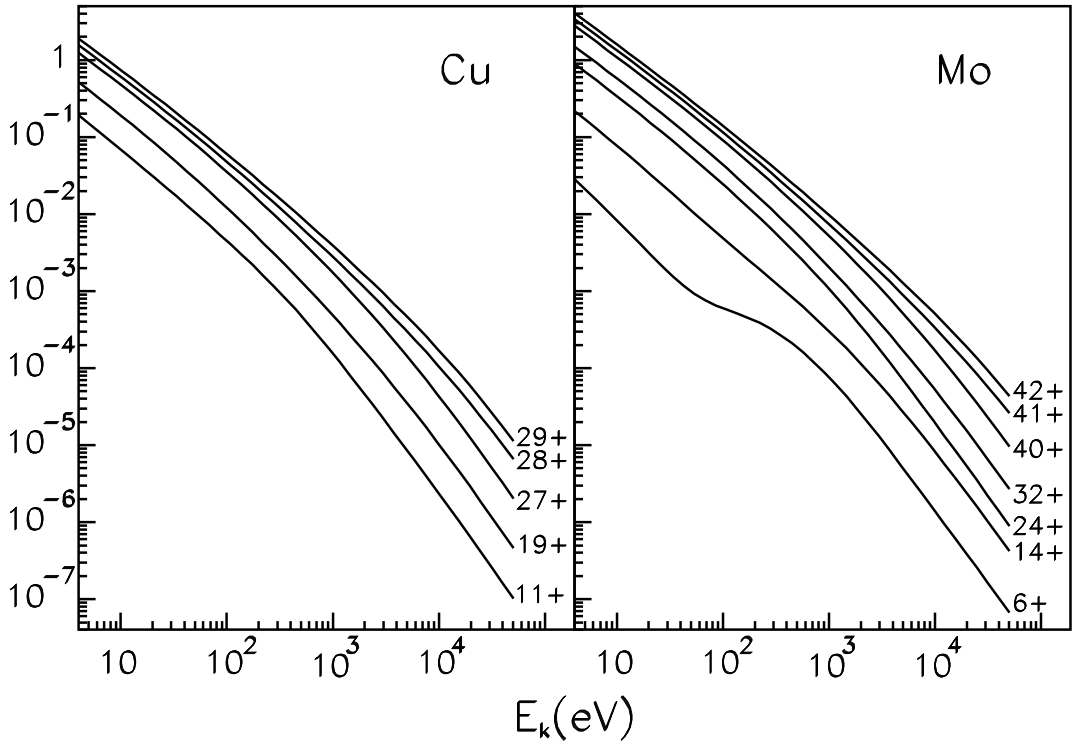

Figure 10: Total RRCS in Mb for ions of Cu and Mo versus E_k.

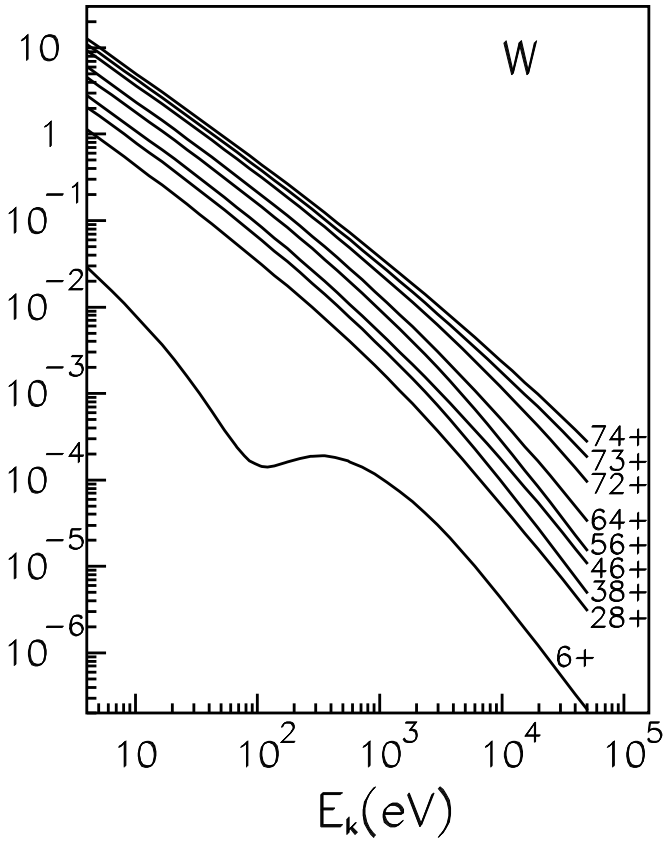

Figure 11: Total RRCS in Mb for ions of W versus E_k.

4 ANALYTICAL FITS OF PHOTOIONIZATION CROSS SECTIONS

A great deal of the subshell RRCS and PCS values produced in the course of calculations may be used thereafter in modern computer codes for handling various problems of plasmas and astrophysics. For this purpose, PCSs are conveniently described by a simple analytical expression with a small number of fit parameters. The parameters permit the subshell RRCS to also be easily obtained using Eq. (5) or Eq. (6).

We applied the procedure developed in [10, 11]. The method is based on the approximate similarity of PCSs for atomic shells with the same n and κ but for different atoms and ions revealed by Kamrukov *et al.* [21]. The criterion can be written as follows:

$$\sigma_{ph}^{(n\kappa)}(k) \;=\; \sigma_0\, F(y)\,, \quad y \;=\; k/k_0\,. \tag{15}$$

Here σ_0 and k_0 are fit parameters depending on quantum numbers n and κ of a shell as well as on Z and N (N is the number of electron in an ion), while $F(y)$ is a so-called "nearly universal" function depending strongly on n and κ and depending weakly on Z and N. Each k-dependent curve of PCS in logarithmic variables, $\log \sigma_{ph}^{(n\kappa)}(\log k)$, may be shifted to a "nearly universal" curve $\log F(y)$. The shift along the energy axis is determined by the fit parameter k_0, while the shift along the PCS axis by the fit parameter σ_0 [10, 11, 21]. A form of the function $F(y)$ furnishing the desired result was proposed in [11] as follows

$$F(y) \;=\; \left[(y-1)^2 + y_w^2\right] y^{-Q} \left(1 + \sqrt{y/y_a}\right)^{-p}, \tag{16}$$

where y_w, y_a and p are three additional fit parameters, and $Q = 5.5 + \ell - 0.5p$. Each of the parameter is responsible for the PCS behavior in a specific range of the photon energy [11].

With Eqs.(15) and (16) the fit parameters were obtained by minimizing the mean-square deviation from calculated values $\sigma_{ph}^{(n\kappa)}$. We used the method of the simplex search developed by Nelder and Mead [22].

For each recombined ion, the fit parameters were calculated for all electron states with quantum numbers $n_{min} \le n \le 12$ and $\kappa = \mp 1, \mp 2, \ldots \mp 6, -7$. The fitting was produced in the photon energy range from $k_{\min} = E_{th} + 4\,\mathrm{eV}$ to $k_{\max}$ where $\sigma_{ph}^{(n\kappa)}(k_{\max})$ falls by five orders of magnitude as compared with its maximum

value, the energy $E_k = k_{\max} - E_{th}$ being less than 50 keV. Usually, $k_{\max}$ is of the order of $100E_{th}$ for the s, p, d, and f shells and $k_{\max}$ is of the order of $10E_{th}$ for the g, h, and i shells. For the very inner shells of the highest-charged ions, $k_{\max}$ may be of the order of several E_{th} in view of the large magnitude of E_{th}. With these fit parameters and Eqs. (15) and (16), one can obtain the value of PCS $\sigma_{ph}^{(n\kappa)}(k)$ per one electron.

For the each shell, we found the relative root-mean-square error δ_{av} as follows:

$$\delta_{av} = \sqrt{\frac{1}{M}\sum_{i=1}^{M}\left[\frac{\sigma_{\rm calc}^{(n\kappa)}(k_i) - \sigma_{\rm fit}^{(n\kappa)}(k_i)}{\sigma_{\rm calc}^{(n\kappa)}(k_i)}\right]^2} \cdot 100\%\,, \tag{17}$$

where $M \leq 41$ is the number of points involved in the fitting, $\sigma_{\rm calc}^{(n\kappa)}(k_i)$ and $\sigma_{\rm fit}^{(n\kappa)}(k_i)$ are values of PCS calculated and obtained in the fitting, respectively.

As a rule, the fitting was carried out with good accuracy and $\delta_{av} \lesssim 2\%$. However there are several cases where the error may be greater. The worst-fitting cases in our calculations are related to the nf shells of the lowest-charged ion W^{5+} revealing a very deep Cooper minimum and to the ns shells of W^{5+} and Mo^{5+}. A comparison between PCSs calculated and obtained by fitting is presented in Fig. 12 for the $ns_{1/2}$ shells of Mo^{5+} and W^{5+} as well as for the $nf_{5/2}$ shells of W^{5+}. Solid lines refer to the fitted $\sigma_{ph}^{(n\kappa)}$ and circles denote PCSs obtained in the DF calculations. The fitting errors δ_{av} are the largest in these three cases. The errors reach $\sim 11\%$ for the $7f$ and $8f$ shells, $\sim 8\%$ for the $10s_{1/2}$ shell of W^{5+}, and $\sim 7\%$ for the $12s_{1/2}$ shell of Mo^{5+}.

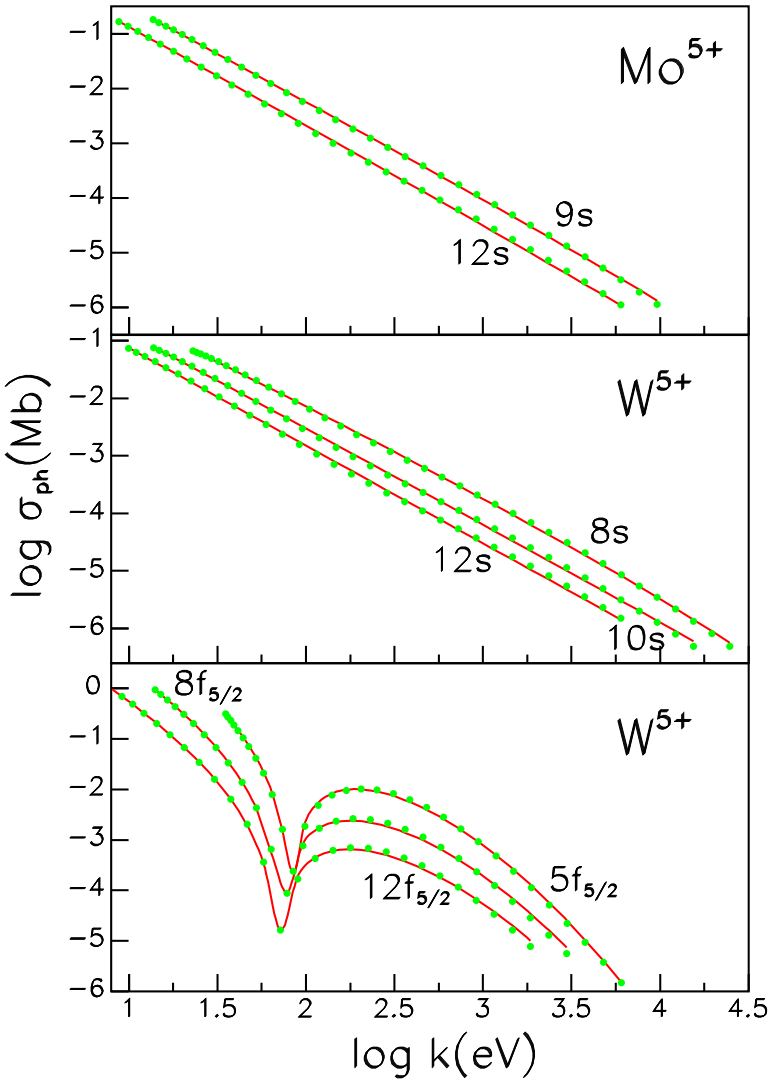

Figure 12: Worst-fitting cases. Fitted (solid lines) and calculated (circles) PCSs versus the photon energy k.

Nevertheless, the fitting error is small for all other shells of Mo^{5+} and W^{5+} including the nd shells (see Fig. 13) where the Cooper minimum exists as well, but not as deep as for the nf shells in W^{5+}. The maximum errors for the nd shells of Mo^{5+} and W^{5+} are $\lesssim 4\%$ and $\lesssim 2\%$, respectively. For shells with the larger orbital quantum number ($\ell > 3$) of the lowest-charged ions as well as for all shells of the higher-charged ions, the fitting accuracy is commonly $\lesssim 1-2\%$.

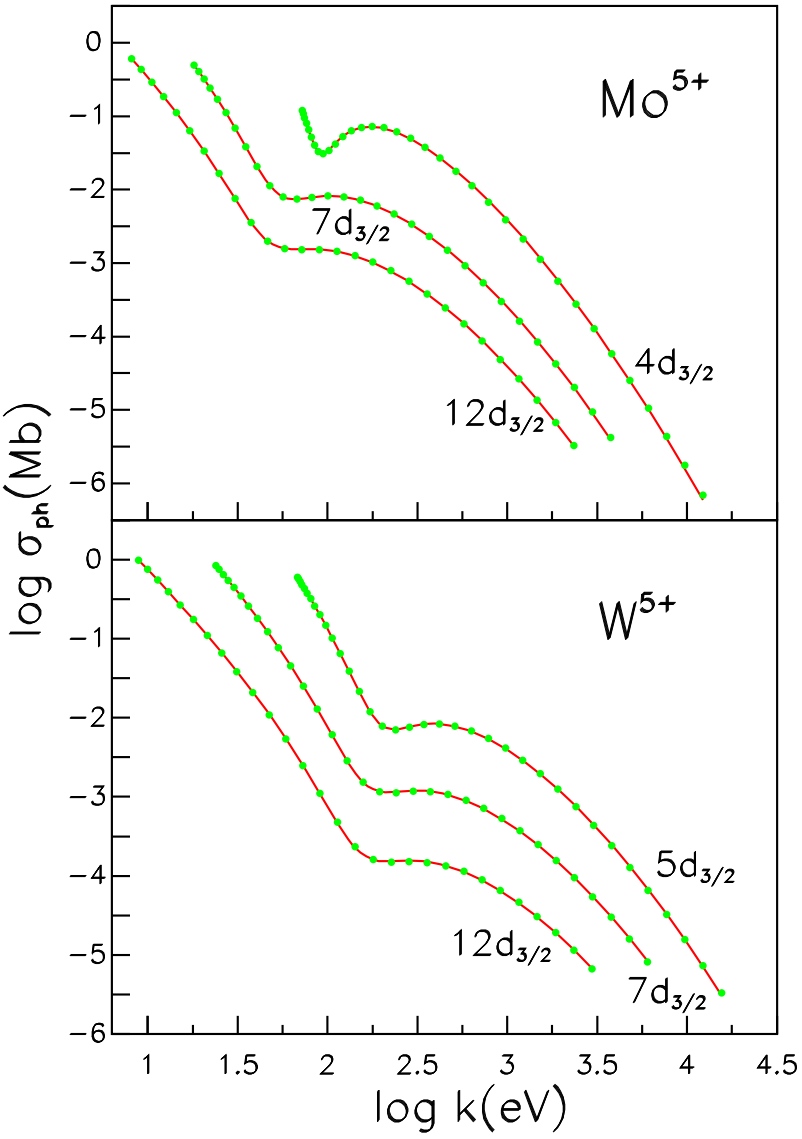

Figure 13: Fitted (solid lines) and calculated (circles) PCSs for the $nd_{3/2}$ shells of Mo^{5+} and W^{5+} versus the photon energy k.

References

[1] I.M. Band, M.B. Trzhaskovskaya, C.W. Nestor,Jr, P.O. Tikkanen, and S. Raman, Atomic Data and Nuclear Data Tables **81**, 1 (2002).

[2] I.M. Band, M.A. Listengarten, M.B. Trzhaskovskaya, and V.I. Fomichev. *Computer program complex RAINE*, I–VI, LNPI Reports LNPI-289 (1976); LNPI-298, LNPI-299, LNPI-300 (1977); LNPI-498 (1979); LNPI-1479(1989).

[3] M.B. Trzhaskovskaya and V.K. Nikulin, Optics and Spectroscopy **95**, 537 (2003).

[4] M. O'Mullane, N.R. Badnell, H.P. Summers, A.D. Whiteford, and M. Witthoeft, *Atomic data and modelling for analysis of heavy impurity behavior in fusion plasmas*. First IAEA Research Co-ordination Meeting "Atomic Data for Heavy Element Impurities in Fusion Reactors", November 2005, IAEA, Vienna; www-amdis.iaea.org/CRP/Heavy_elements/Presentations/

[5] J.H. Scofield, J. Electron Spectrosc. Relat. Phenom. **8**, 129 (1976).

[6] J.H. Scofield, Phys. Rev. A**40**, 3054 (1989).

[7] I.M. Band, Yu.I. Kharitonov, and M.B. Trzhaskovskaya, Atomic Data and Nuclear Data Tables **23**, 443 (1979).

[8] J.J. Yeh and I. Lindau, Atomic Data and Nuclear Data Tables **32**, 1 (1985).

[9] M.B. Trzhaskovskaya, V.I. Nefedov, and V.G. Yarzhemsky, Atomic Data and Nuclear Data Tables **77**, 97, 2001; *ibid.:* **82**, 257, 2002.

[10] I.M. Band, M.B. Trzhaskovskaya, D.A. Verner, and D.G. Yakovlev, Astron. Astrophys. **237**, 267 (1990).

[11] D.A. Verner, D.G. Yakovlev, I.M. Band, and M.B. Trzhaskovskaya, Atomic Data and Nuclear Data Tables **55**, 233 (1993).

[12] D.A. Verner and G.J. Ferland, Ap. J. Suppl. **103**, 467 (1996).

[13] M.F. Gu, ApJ **589**, 1085 (2003).

[14] Sultana N. Nahar and Anil K. Pradhan, Radiation Physics and Chemistry **70**, 323 (2004).

[15] Sultana N. Nahar and Anil K. Pradhan, Astrophys. J. Suppl. Series, **162**, 417 (2006).

[16] Sultana N. Nahar, Anil K. Pradhan, and Hong Lin Zhang, Astrophys. J. Suppl. Series, **133**, 255 (2001).

[17] A. Ichihara and J. Eichler, Atomic Data and Nuclear Data Tables **74**, 1 (2000).

[18] N.R. Badnell, Astrophys. J. Suppl. Series, **167**, 334 (2006).

[19] I.P. Grant, Adv.Phys. **19**, 747 (1970).

[20] H.A. Bethe and E.E. Salpeter, *"Quantum Mechanics of One- and Two-Electron Atoms"* (Springer-Verlag, Berlin, 1957) Chapter IV.

[21] A.S. Kamrukov, N.P. Kozlov, Yu.S. Protasov, and S.N. Chuvashev, Opt. Spectroscopy **55**, 17 (1983).

[22] D.M. Himmelblau, *"Applied nonlinear programming"* (McGraw-Hill, 1972) p. 163.